Time Projection Chambers

D. Kahl, Y. Xu, H. Yamaguchi, D. Balabanski, U. Battino, O. Beliuskina, S. M. Cha, K. Y. Chae, A.A. Chen, M. Cuciuc, M. Cwiok, W. Dominik, M. Gai, L.-B. Galadriel, G.L. Guardo, T. Hashimoto, S. Hayakawa, G. Kaminski, A. Kankainen, C. Kim, M. Kim, S. Kim, M. La Cognata, L. Lamia, D. Lattuada, C. Matei, S. Palmerini, R.G. Pizzone, S. Romano, P.-A. Söderström, D.K. Schweitzer, M. Sferrazza, R. Smith, S.R. Stern, D. Testov, A. Tumino, and V. Vasilca

October 25, 2021; `david.kahl@eli-np.ro`

Extreme Light Infrastructure – Nuclear Physics, IFIN-HH

Presented at New Trends in Nuclear Physics Detectors, HIL, Warsaw

Outline

1) Astrophysical abundances
2) X-ray Bursts
3) CRIB laboratory, Tokyo
4) My PhD work with an active target
5) What is a TPC, anyway?
6) *s*-process and importance of ^{22}Ne(α, n)
7) Introduction to the ELI-NP miniTPC device
8) New approved experiment at IFIN-HH 9 MV tandem

what elements are mostly in the universe. . . ?

Astronomer's Periodic Table

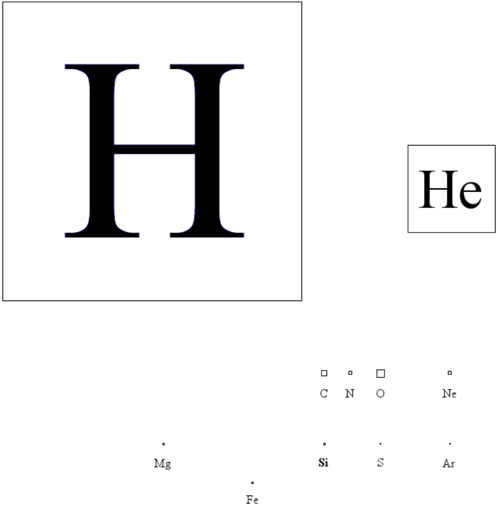

Figure: Baryonic mass of the universe >99% hydrogen and helium.

Inspired by Ben McCall, Jason Tumlins, Jim Truran, and others from University of Chicago.

how does hydrogen burn. . .

Carbon-Nitrogen-Oxygen Catalytic Cycles

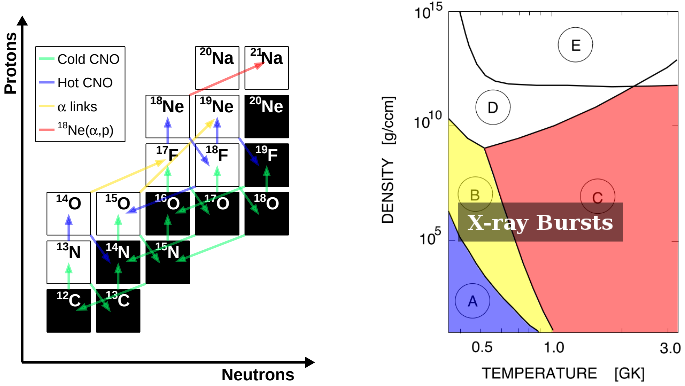

(a) Schematic of CNO Cycles (b) T vs. ρ plot

Figure: (a) the reaction pathways which dominate according to stellar conditions of (b): HCNO cycles operate in Ⓐ. $^{14}\mathrm{O}(\alpha,p)^{17}\mathrm{F}$ and $^{15}\mathrm{O}(\alpha,\gamma)^{19}\mathrm{Ne}$ operate in Ⓑ. $^{18}\mathrm{Ne}(\alpha,p)^{21}\mathrm{Na}$ breakout operates in Ⓒ.

(b) modified from Wiescher, M., Görres, J. & Schatz, H., TOPICAL REVIEW: Break-out reactions from the CNO cycles, Journal of Physics G Nuclear Physics **25** (1999) 133–161

accretion is mass transfer...

Thermonuclear runaway from accretion

- *Novae* occur in accreting *white dwarf* binaries
- *X-ray bursts* occur in accreting *neutron star* binaries
- The companion star should be near a solar mass, $M_\odot$
  - Required for Roche lobe overflow
- High local gravity $g \rightarrow$ high pressure P
- High impacting velocity v
- High temperature T
- Fresh supply of H and He (nuclear fuel)
- e^- degenerate matter leads to explosive burning
  - P only weakly depends on T
- Thermonuclear runaway!
- Binary star system
  - 50% of all star systems
  - Compact-object binaries are fewer

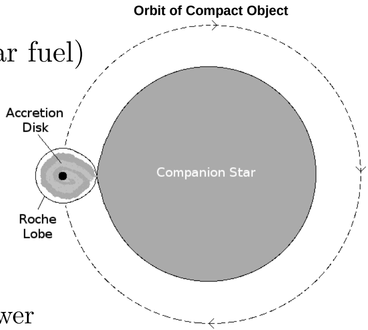

XRB spectra look like...

Observations of X-ray Bursts (∼100 known systems)

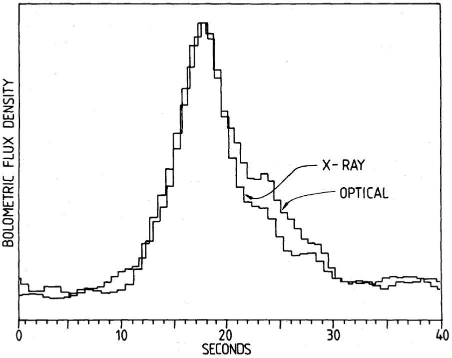

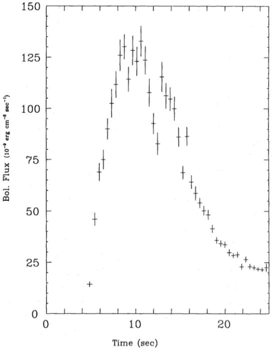

Models should reproduce the observable structure of bursts

Accretion on a Neutron Star. . . is exciting!

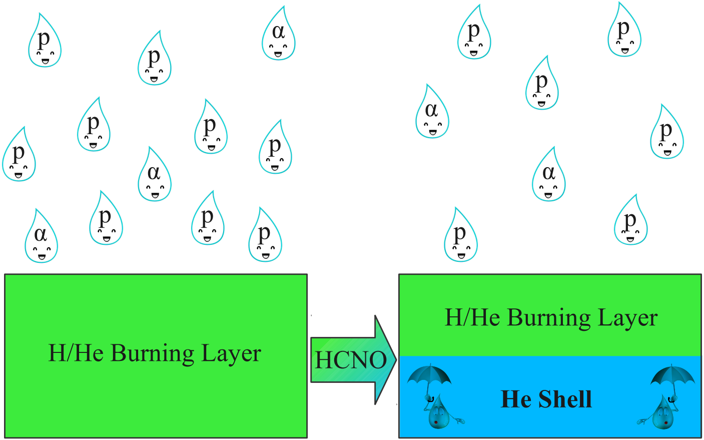

H/He Shell Flash

$\uparrow \dot{M}$ means $\downarrow t_{burst}$ & $\downarrow L_{burst}$

Pure He Shell Flash

$\downarrow \dot{M}$ means $\uparrow t_{burst}$ & $\uparrow L_{burst}$

Helium is pretty explosive. . .

Example of neutron-deficient explosive He burning

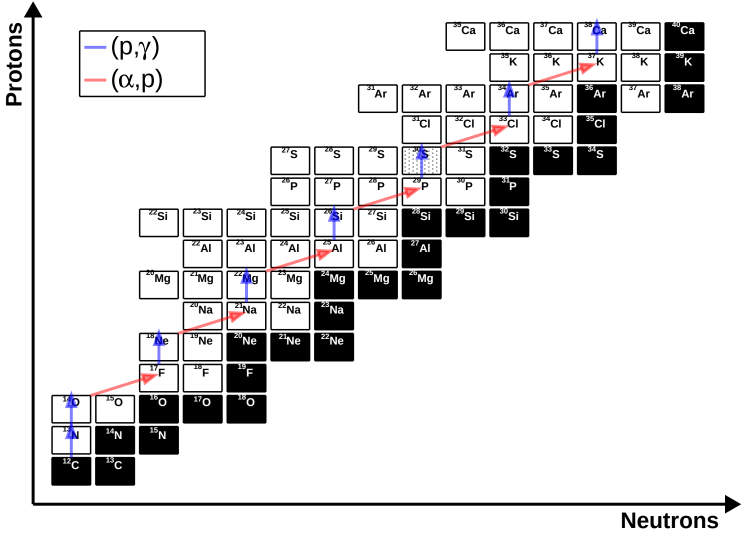

Figure: One of the αp-process pathways. We investigated ^{18}Ne(α, p), ^{22}Mg(α, p) and ^{30}S(α, p) at CRIB with the active target.

and there is an experiment for this, too. . .

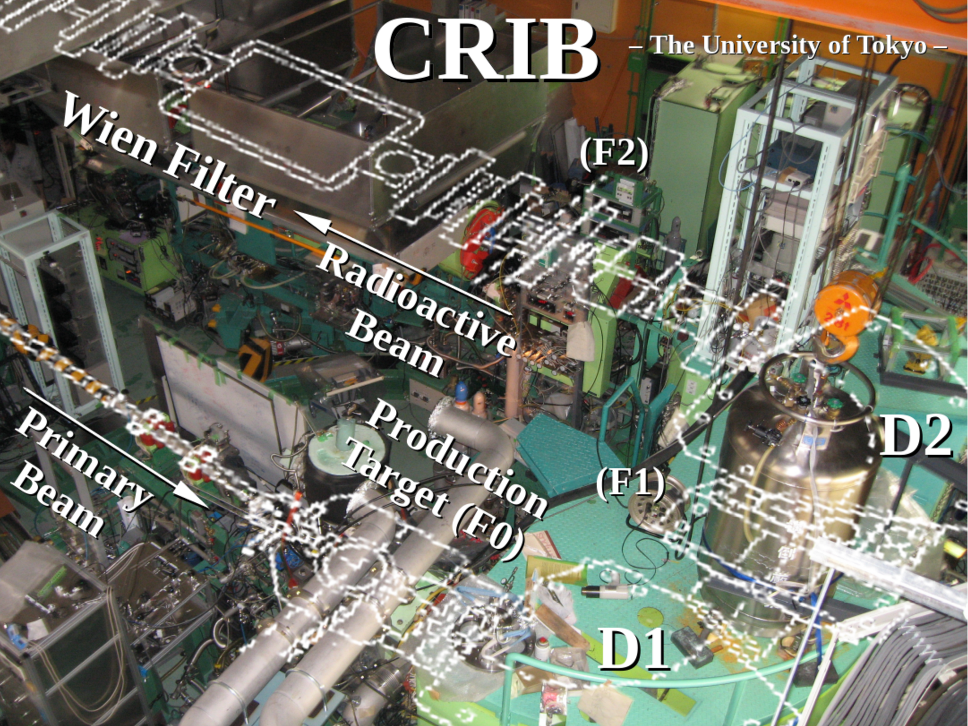
CRIB
– The University of Tokyo –
Wien Filter
(F2)
Radioactive Beam
Production Target (F0)
Primary Beam
(F1)
D2
D1

For details, please see our magazine article

Nuclear Physics News

ISSN: 1061-9127 (Print) 1931-7336 (Online) Journal homepage: https://www.tandfonline.com/loi/gnpn20

CRIB: The Low Energy In-Flight RI Beam Separator

Hidetoshi Yamaguchi, Daid Kahl & Shigeru Kubono

To cite this article: Hidetoshi Yamaguchi, Daid Kahl & Shigeru Kubono (2020) CRIB: The Low Energy In-Flight RI Beam Separator, Nuclear Physics News, 30:2, 21-27, DOI: 10.1080/10619127.2020.1717263

Hidetoshi Yamaguchi
CNS, University of Tokyo

Daid Kahl
University of Edinburgh

Shigeru Kubono
RIKEN

- Aimed at a general audience in nuclear physics
  - Overview of in-flight radioactive beam production
  - Highlights of our more recent works
- Check out www.nupecc.org for similar articles!

PHYSICAL REVIEW C **97**, 015802 (2018)

First measurement of ^{30}S + α resonant elastic scattering for the ^{30}S(α, p) reaction rate

D. Kahl,[1,2,*] H. Yamaguchi (山口英斉),[1] S. Kubono (久保野茂),[1,3,4] A. A. Chen,[5] A. Parikh,[6] D. N. Binh,[1,†] J. Chen (陈俊),[5,‡] S. Cherubini,[7,8] N. N. Duy,[9,10,§] T. Hashimoto (橋本尚志),[1,‖] S. Hayakawa (早川勢也),[1] N. Iwasa (岩佐直仁),[11] H. S. Jung (정효순),[12] S. Kato (加藤静吾),[13] Y. K. Kwon (권영관),[12,‖] S. Nishimura (西村俊二),[3] S. Ota (大田晋輔),[1] K. Setoodehnia,[5,¶] T. Teranishi (寺西高),[14] H. Tokieda (時枝紘史),[1] T. Yamada (山田拓),[11,#] C. C. Yun (윤종철),[12,‖] and L. Y. Zhang (张立勇)[4,**]

^{30}S radioactive beam injected into an active target

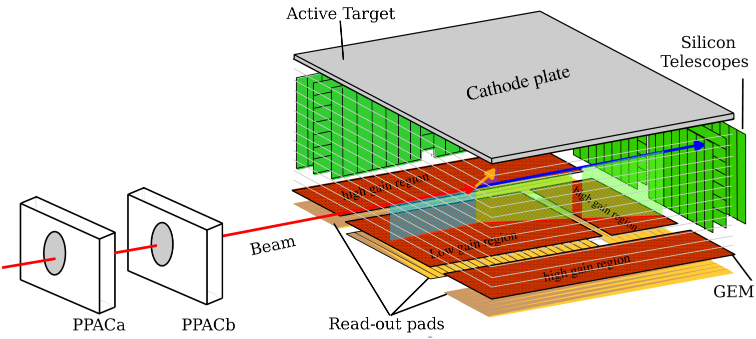

here are some details. . .

What is a Time Projection Chamber (TPC)?

1) It's just an ionization chamber, old technology in principle
2) Gas-filled detector
3) Gas-filled target – good for astrophysics
4) We can determine X, Y, Z, ΔE (and E, depending)
5) Essentially 4π coverage for charged particles
6) Difficult to design correctly and operate
6) Use monoenergetic source to test, *e.g.* ^{241}Am

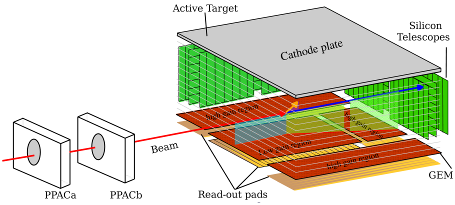

(a) Schematic

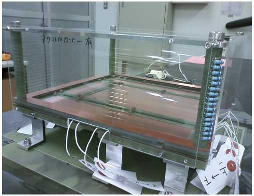
(b) Photograph

so we can look at the components...

GEM – MSTPC Multiple Sampling and Tracking Proportional Chamber with Gas Electron Multiplier

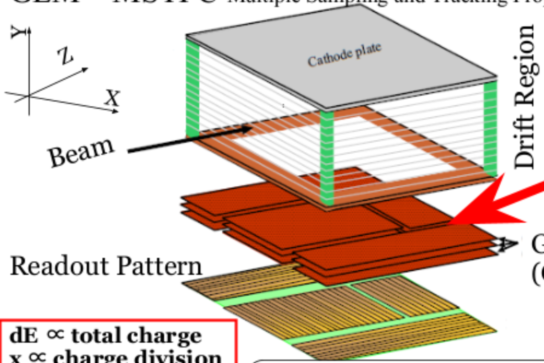

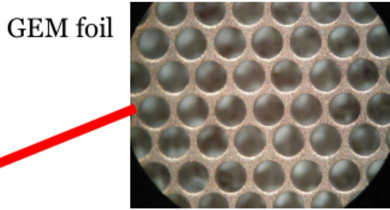

dE ∝ total charge
x ∝ charge division
y ∝ drift time
z ∝ pad number

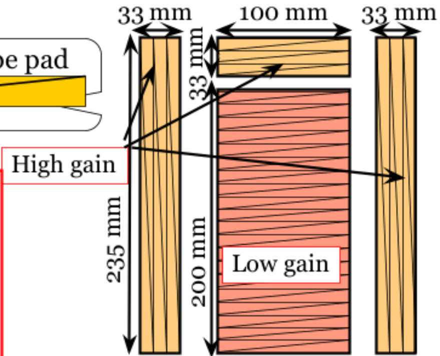

Requirements

Gas gain : low gain region 10^3
high gain region 10^5
Long time stability
High rate beam injection capability
Energy resolution : <10%
position resolution : < 2mm

Basics of TPC operation with GEM

- Electronic Time Projection Chamber (TPC)
- Drift time of electrons around μs per cm
  - Limits event rate to around 10^6 / second
- Gas Electron Multiplier (GEM) foils
- 90% He + CO_2 at 25% atm
- Low pressure gas has a high dielectric constant – sparks!
- GEM gas gain goes linearly then exponentially with bias

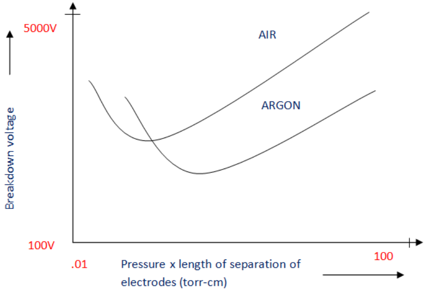

(a) electrical4u.com

Top	-2828	Bottom	-1000
Low-gain		High-gain	
Cover	-950	—	—
1U	-913	—	—
1D	-823	Cover	-992
2U	-803	1U	-899
2D	-587	1D	-694
3U	-513	2U	-655
3D	-135	2D	-135

(b) Biases for ^{30}S+α

The tail of two cats

- There are many ways around injection / event limit
  - Bridges…
  - Two field cages!
- CNS Active Target = CAT
- Shinsuke OTA was heading up this research (UTokyo)
  - (α, α') and $(d, 2p)$ for GT

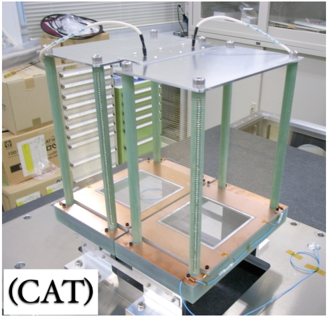

(a) Twin field cages!

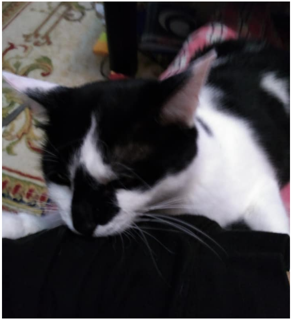

(b) Galadriel bites Sarah!

Flash ADC type sampling readout

- Record full waveform of analog signal
- Lots of data, sampling at 10s of MHz typically
- Baseline subtraction is possible
- Peak finding algorithm required: moving average technique
  - github.com/goatface/crabat/Analyzer.cxx line 1670
- Contamination by air: terrible waveforms
- Contamination by water vapor: sparks
- New GET electronics really simplfy this setup

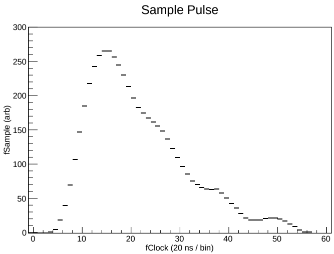

(a) 'Nice' pulse (but still wavy)

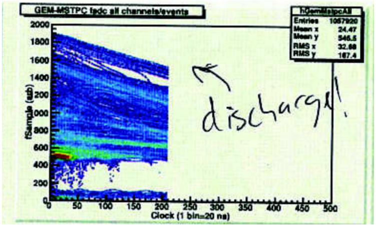

(b) 10^{-5} N_2 destroys pulses

examples of why GET system is better and compact...?


注意！！
赤ランプ 点滅時
高電圧印加中
High Voltage


高電圧印加中
High Voltage
注意！！

Be careful with energy loss from SRIM at low energy

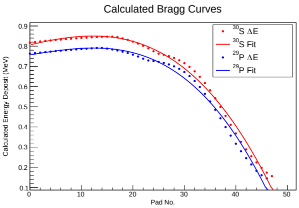

(a) **enewz** wobbles but nice

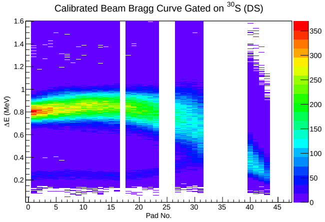

(b) Data are smooth

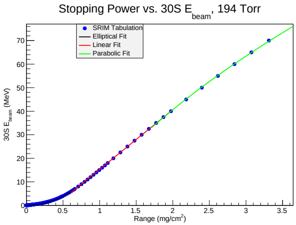

(c) SRIM is tricky to fit

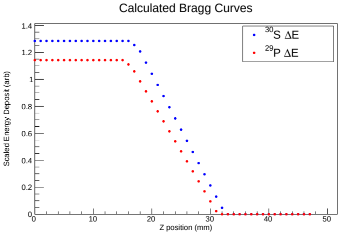

(d) SRIM has unrealistic kinks

time to look at some TPC tracks. . . ?

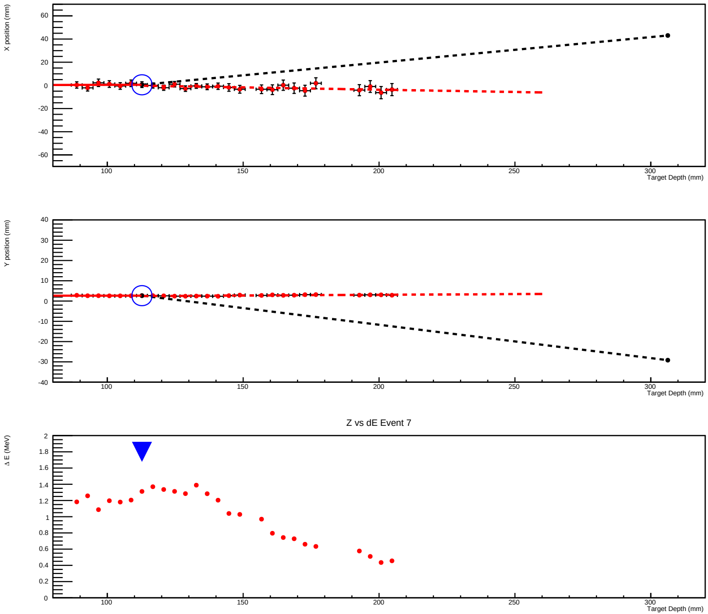

Better to explain carefully how the algorithm works. . .

Scattering Location By Beam Tracking

- After data processing and gating, we have two possibilities:
  - **1) Upstream scattering**
    - (This is the 83 mm of target gas before the active region)
    - We should find a good single linear fit in X and Y
    - There is no relation with the PPAC data
  - **2) Active target scattering**
    - We should find two pairs of linear fits in X and Y
    - The vertex must be the same
    - The first sets of linear fits include the PPAC data
    - There should be a local increase in ΔE at the vertex
- In both cases, the slopes must go opposite of the α
- Compute and compare χ^2_ν to distinguish **1** & **2**
  - If $\left(\left({}_{\mathbf{1}}\chi^2_\nu < {}_{\mathbf{2}}\chi^2_\nu\right) \textit{ and } \left({}_{\mathbf{2a}}\chi^2_\nu > 1 \textit{ or } {}_{\mathbf{2b}}\chi^2_\nu > 1\right)\right)$: upstream
  - Else as long as all $\chi^2_\nu < 1$: active target case)
    - This is because of additional ΔE constraint
- Let's see how well it works!

After having the idea, several more events...

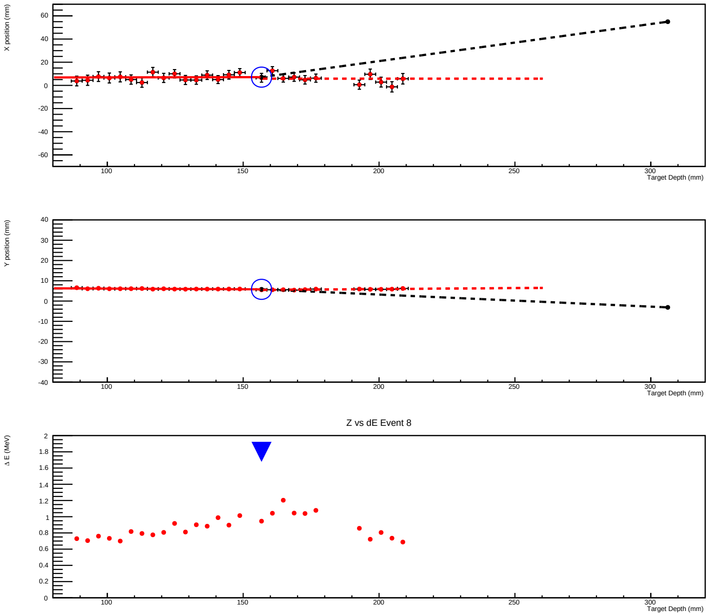
X position (mm)
60
40
20
0
-20
-40
-60
100
150
200
250
300
Target Depth (mm)
Y position (mm)
40
30
20
10
0
-10
-20
-30
-40
Z vs dE Event 8
Δ E (MeV)
2
1.8
1.6
1.4
1.2
1
0.8
0.6
0.4
0.2
0

more events. . .

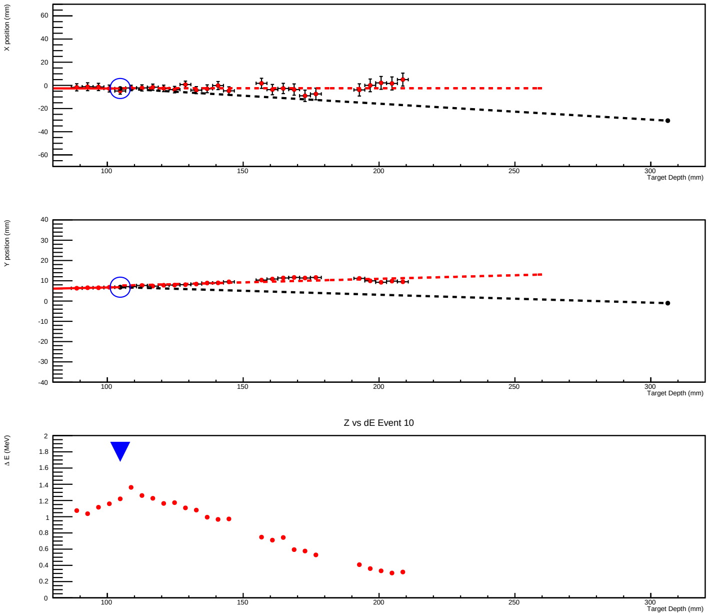
X position (mm)
Target Depth (mm)
Y position (mm)
Target Depth (mm)
Z vs dE Event 10
Δ E (MeV)
Target Depth (mm)

more events. . .

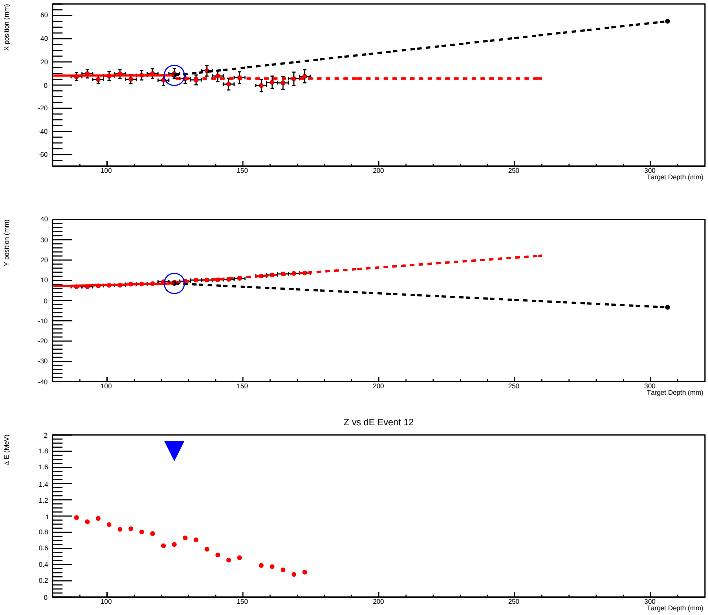
X position (mm)
60
40
20
0
-20
-40
-60
100
150
200
250
300
Target Depth (mm)
Y position (mm)
40
30
20
10
0
-10
-20
-30
-40
100
150
200
250
300
Target Depth (mm)
Z vs dE Event 12
Δ E (MeV)
2
1.8
1.6
1.4
1.2
1
0.8
0.6
0.4
0.2
0
100
150
200
250
300
Target Depth (mm)

more events. . .

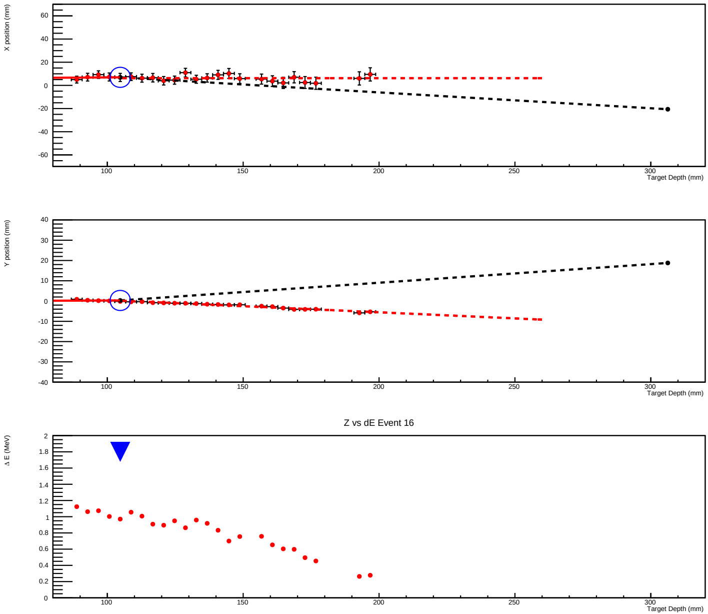

X position (mm)
60
40
20
0
-20
-40
-60
100
150
200
250
300
Target Depth (mm)
Y position (mm)
40
30
20
10
0
-10
-20
-30
-40
100
150
200
250
300
Target Depth (mm)
Z vs dE Event 16
Δ E (MeV)
2
1.8
1.6
1.4
1.2
1
0.8
0.6
0.4
0.2
0
100
150
200
250
300
Target Depth (mm)

more events. . .

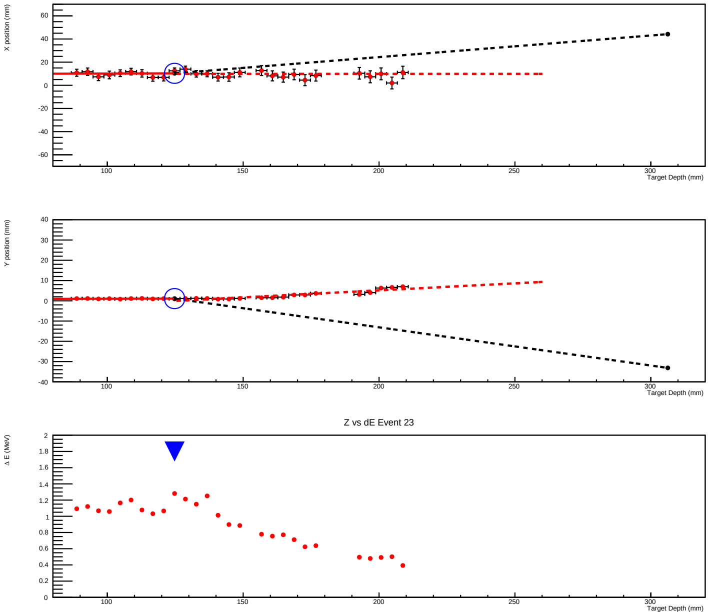
X position (mm)
Y position (mm)
Z vs dE Event 23
Δ E (MeV)
Target Depth (mm)

more events. . .

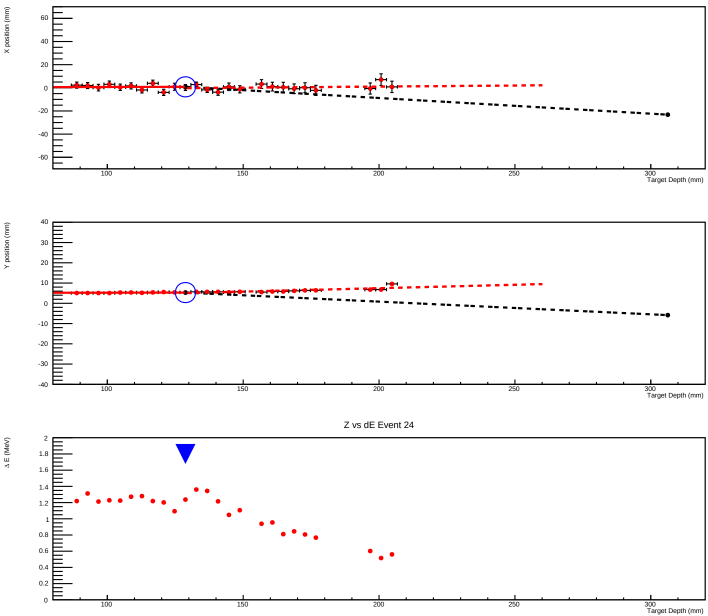
X position (mm)
60
40
20
0
-20
-40
-60
100
150
200
250
300
Target Depth (mm)
Y position (mm)
40
30
20
10
0
-10
-20
-30
-40
100
150
200
250
300
Target Depth (mm)
Z vs dE Event 24
Δ E (MeV)
2
1.8
1.6
1.4
1.2
1
0.8
0.6
0.4
0.2
0
100
150
200
250
300
Target Depth (mm)

more events. . .

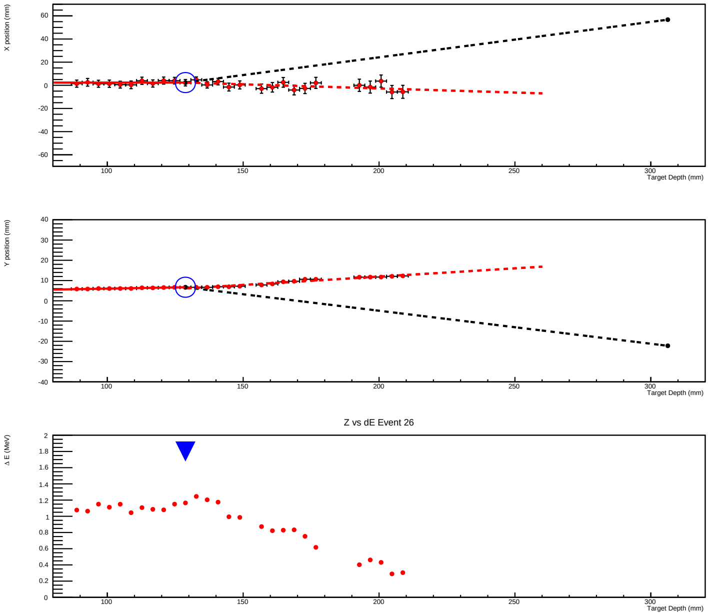
X position (mm)
60
40
20
0
-20
-40
-60
100
150
200
250
300
Target Depth (mm)
Y position (mm)
40
30
20
10
0
-10
-20
-30
-40
Target Depth (mm)
Z vs dE Event 26
Δ E (MeV)
2
1.8
1.6
1.4
1.2
1
0.8
0.6
0.4
0.2
0
Target Depth (mm)

more events. . .

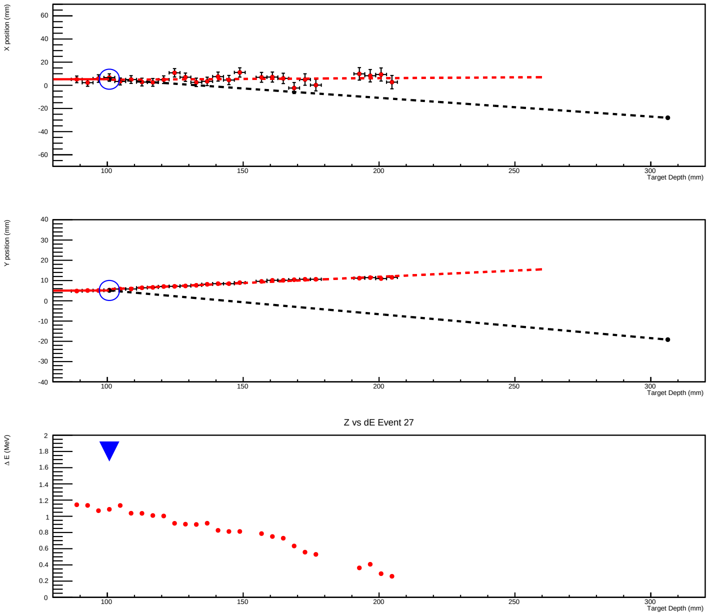

X position (mm)
Y position (mm)
Z vs dE Event 27
Δ E (MeV)
Target Depth (mm)

more events. . .

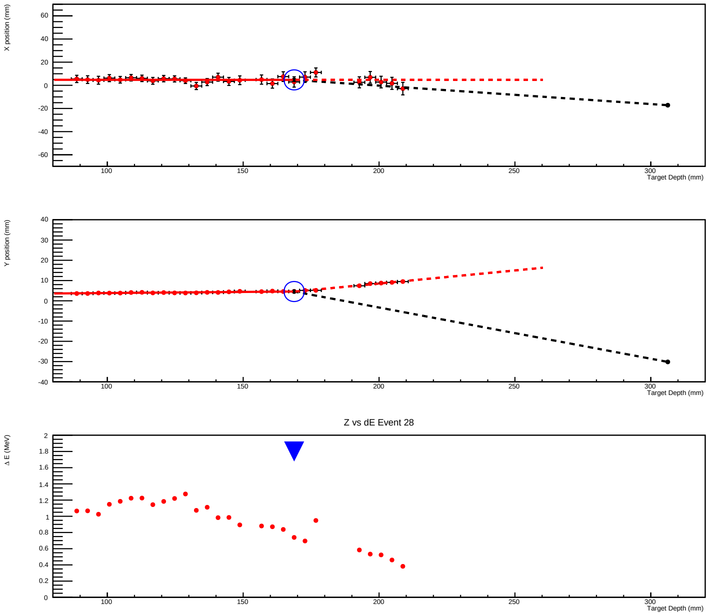

X position (mm)
60
40
20
0
-20
-40
-60
100
150
200
250
300
Target Depth (mm)
Y position (mm)
40
30
20
10
0
-10
-20
-30
-40
100
150
200
250
300
Target Depth (mm)
Z vs dE Event 28
Δ E (MeV)
2
1.8
1.6
1.4
1.2
1
0.8
0.6
0.4
0.2
0
100
150
200
250
300
Target Depth (mm)

more events. . .

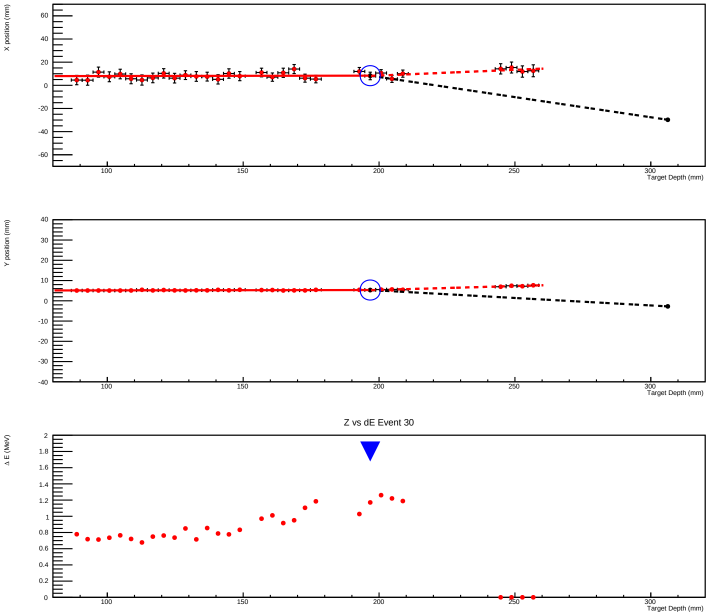
X position (mm)
Y position (mm)
Z vs dE Event 30
Δ E (MeV)
Target Depth (mm)

more events. . .

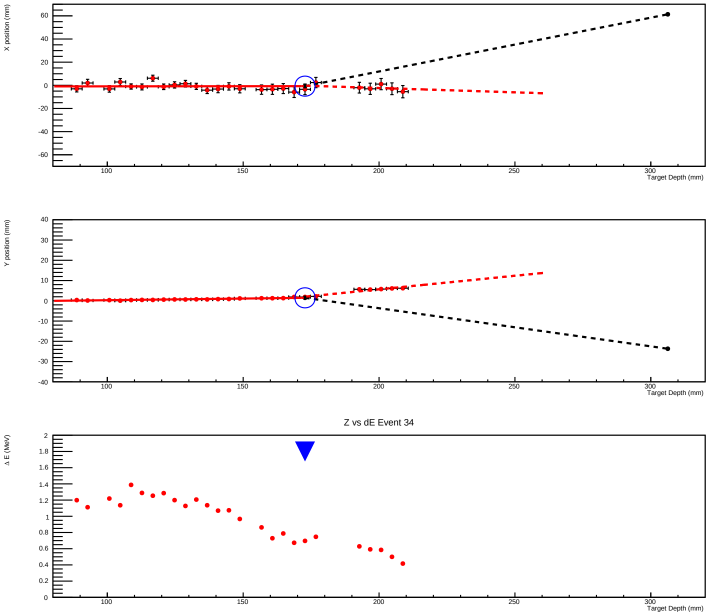

summing them all up. . .

Beam X residual ^{30}S and ^{29}P before gain calibration

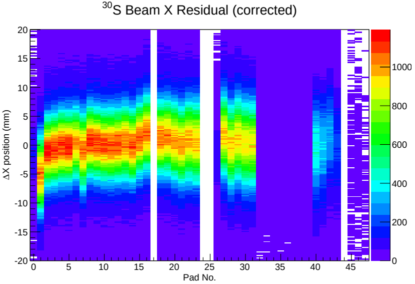

(e) ΔX Residual for ^{30}S

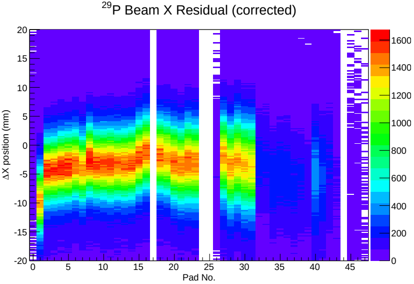

(f) ΔX Residual for ^{29}P

Figure: Geometric correction is made, and then ΔX is determined by the active target position minus the PPAC extrapolation. But the position determination shows some non-linearity, since ^{29}P is non-central and active target data suggests it is closer to the center than the actual case. ^{30}S is injected over the central region.

Though the calibrated spectrum looks much nicer. . .

Unscattered beam tracking by charge-division for ^{30}S

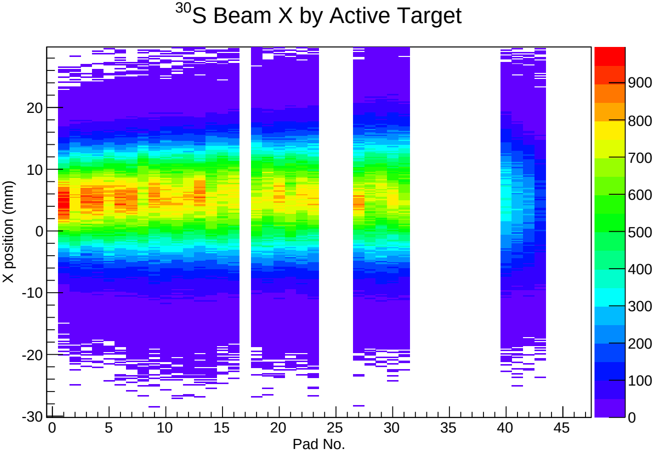

Figure: ^{30}S beam track in X over the low-gain active target region. Beam penetration depth (left to right) with pad number(4 mm) vs. left/right position derived by charge-division.

Comparing with a simulation yields the resolution of. . .

Beam X residual ^{30}S

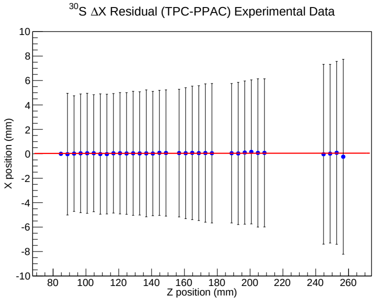

(a) ΔX Residual by Experiment

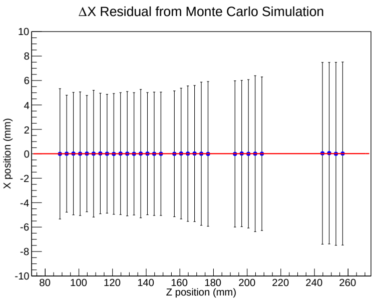

(b) ΔX Residual by Simulation

Figure: Projection and fit of the beam residual data for X position. ΔX is determined by the active target position minus the PPAC extrapolation. TPC resolution by charge-division ranges from 3 mm to 5.5 mm depending on ΔE. PPAC resolution is 0.9 mm. Errors are 1σ.

Unscattered beam tracking by drift-time for ^{30}S

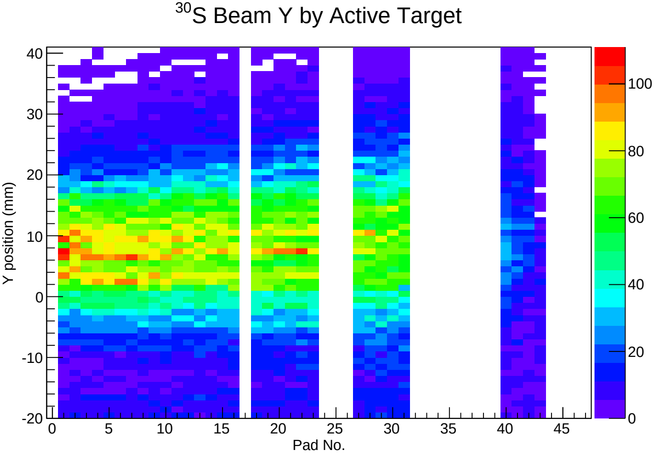

Figure: ^{30}S beam track in Y over the low-gain active target region. Beam penetration depth (left to right) with pad number(4 mm) vs. up/down position derived by electron drift time.

Comparing with a simulation yields the resolution of. . .

Beam Y residual

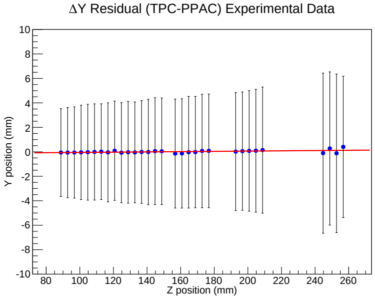

(a) ΔY Residual by Experiment

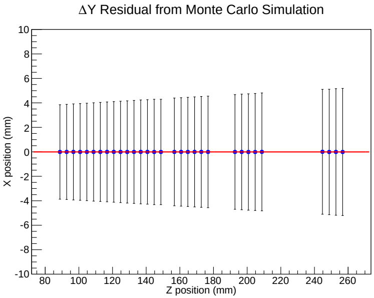

(b) ΔY Residual by Simulation

Figure: Projection and fit of the beam residual data for Y position. ΔY is determined by the active target position minus the PPAC extrapolation. TPC resolution for drift time is 0.5 mm. PPAC resolution is 0.9 mm. Errors are 1σ.

And the results look like. . .

Track finding: Garbage in, garbage out

- Resolution was not good enough to find tracks
- Without beam tracking data it was a Gaussian
  - I made a very expensive RNG with an RIB
  - Sorry I couldn't find the figure, I wanted to forget that
- Kinematic solution finds the Rutherford peak: correct
- Trust the measured ΔE; forget the TPC tracks

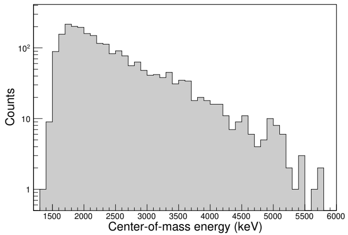

(a) Kinematic solution: right

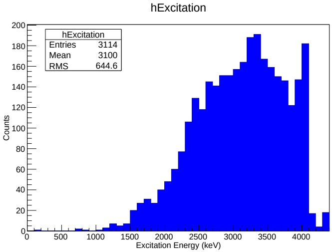

(b) Track finding: wrong

$^{30}S(\alpha, \alpha)$ at CRIB

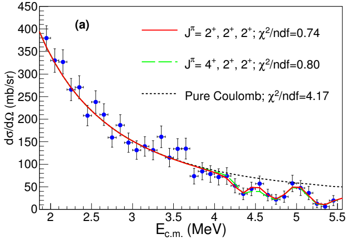

(a) My PhD data†

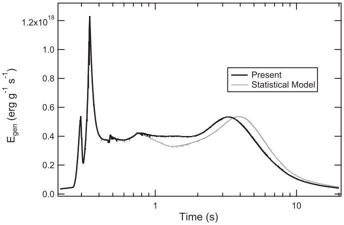

(b) Anuj's post-processing model

- Low-energy ^{30}S RIB at 10^4 pps: 4+ years to develop
- Active target system with He+CO_2 (90% + 10%)
- We found several **huge** resonances with $\theta_\alpha^2 > 40\%$
- Recent work* has assumed $\mathcal{S}_\alpha \approx 0.01$ in any case
- New XRB astrophysical paper in preparation (it's a secret!)

† D. Kahl, H. Yamaguchi, S. Kubono, A. A. Chen, *et al.* Phys. Rev. C **97** (2018) 015802.
* A. M. Long *et al.* Phys. Rev. C **97** (2018) 054613.

^{22}Ne(α, n) is responsible for much of $60 \lesssim A \lesssim 90$

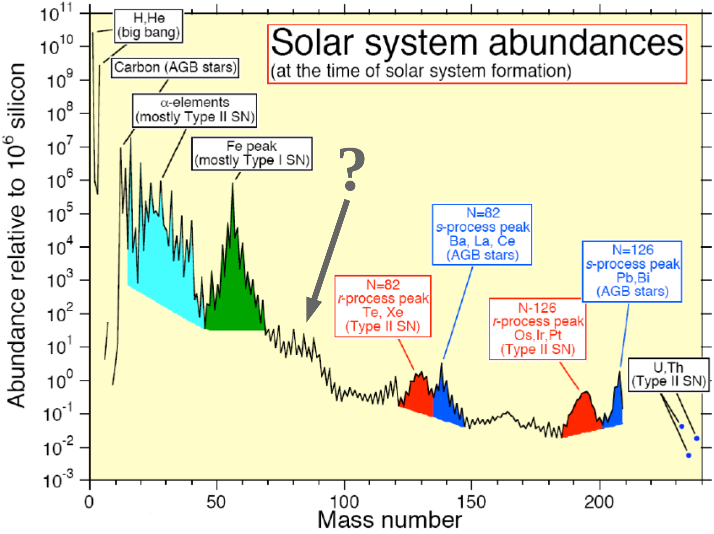

Figure: Absolute abundances of 'weak' s-process $\gg$ 'main' s-process.

Image credit: A. Davis of University of Chicago. Modified by DK for ↙ ?

what's going on near that question mark. . . ?

Nucleosynthesis in $60 \lesssim A \lesssim 90$ is both r- & s-process

- The r-process is a hot topic because of neutron star mergers
- Usually, $r = 1 - s$ for several reasons:
  1) We can generally neglect p-process contributions
  2) We know the sites and stellar models, basically
- $\therefore$ to understand r we need to know s precisely

TABLE 10

Solar System s- and r-Process Abundances

Element (1)	Z (2)	N_{tot} (3)	N_r (4)	$\log \epsilon_r$ [a] (5)	N_s (6)	$\log \epsilon_s$ [a] (7)	r-Fraction (8)	s-Fraction (9)
Ga.................	31	37.850	16.300	2.752	21.550	2.873	0.431	0.569
Ge.................	32	108.757	56.170	3.290	52.587	3.261	0.516	0.484
As.................	33	6.786	5.330	2.267	1.456	1.703	0.785	0.215
Se.................	34	61.443	40.260	3.145	21.183	2.866	0.655	0.345
Br.................	35	5.569	4.640	2.207	0.929	1.508	0.833	0.167
Kr.................	36	51.952	22.680	2.896	29.272	3.006	0.437	0.563
Rb.................	37	5.794	2.890	2.001	2.904	2.003	0.499	0.501
Sr.................	38	23.090	2.550	1.947	20.540	2.853	0.11	0.89
Y.................	39	4.654	1.310	1.657	3.344	2.064	0.281	0.719
Zr.................	40	10.703	2.040	1.850	8.663	2.478	0.191	0.809

Figure: r- & s-Fractions are shuffled near mass numbers 60 to 90

J. Simmerer, *et al.*, ApJ, "The Rise of the s-Process In the Galaxy", **617** (2004) 1091.

what are the known nuclear structure data. . . ?

^{22}Ne(α, n) Part I: ^{26}Mg states with measured Γ_α or $\omega\gamma$

- Many states have discrepant data (not shown here)

E_x (MeV)	E_r^{CM} (keV)	J^π	$\omega\gamma_{(\alpha,\gamma)}$ (eV)	$\omega\gamma_{(\alpha,n)}$ (eV)	Γ_α (eV)	Γ_γ (eV)	Γ_n (eV)	Integrate resonance?
10.6963(4)	81.6(4)	4^+			$3.5(18) \times 10^{-46}$	3.0(15)	0	No
11.084(1)	469(1)	2^+			$5.7(1.5) \times 10^{-11}$	3.0(15)	0	No
11.321(1)	706(1)[a]	$0^+/1^-$	$3.7(4) \times 10^{-5}$	$4.2(11) \times 10^{-5}$				No
11.44120(4)	826.46(5)	3^-		$3.9(10) \times 10^{-5}$	$5.50(14) \times 10^{-6}$	3.0(15)	$1.47(8) \times 10^3$	Yes
11.46574(6)	851.00(6)	3^-		$5.5(17) \times 10^{-5}$	$7.9(2.4) \times 10^{-6}$	3.0(15)	$6.55(9) \times 10^3$	Yes
11.5080(9)	893.3(9)	1^-		$3.5(6) \times 10^{-4}$	$1.2(4) \times 10^{-4}$	3.0(15)	$1.27(25) \times 10^3$	Yes
11.5260(15)	911.3(15)	1^-		$1.3(4) \times 10^{-3}$	$4.3(11) \times 10^{-4}$	3.0(15)	$1.80(25) \times 10^3$	Yes
11.630(1)	1015.3(14)	1^-		$7.1(15) \times 10^{-3}$	$2.4(5) \times 10^{-3}$	3.0(15)	$13.5(17) \times 10^3$	Yes
11.749(5)	1133(6)	1^-		$5.9(8) \times 10^{-2}$	$2.0(3) \times 10^{-2}$	3.0(15)	$64(9) \times 10^3$	Yes
11.787(3)	1172(3)	1^-		$2.5(9) \times 10^{-2}$	$8(3) \times 10^{-3}$	3.0(15)	$24.5(24) \times 10^3$	Yes
11.828(1)	1213(1)	2^+		$2.5(3) \times 10^{-4}$	$1.8(1) \times 10^{-1}$	3.0(15)	$1.10(25) \times 10^3$	Yes
11.863(3)	1248(3)	1^-			$1.5(10) \times 10^{-2}$	3.0(15)	$2.45(34) \times 10^4$	Yes
11.880(3)	1265(3)	1^-		$1.9(19) \times 10^{-1}$	$6.30(63) \times 10^{-2}$	3.0(15)	$3.0(15) \times 10^3$	No
11.895(4)	1280(4)	1^-	$2.0(2) \times 10^{-3}$	$4.1(4) \times 10^{-1}$				No
11.911(1)	1297(3)	1^-	$3.4(4) \times 10^{-3}$	1.4(1)	1.9(9.8)	3.0(15)	$5(2) \times 10^3$	Yes
11.953(3)	1338(3)	2^+	$3.4(4) \times 10^{-3}$	1.60(13)	$3.2(1.7) \times 10^{-1}$	3.0(15)	$2(1) \times 10^3$	Yes
12.050(1)	1436(3)	2^+	$6.0(7) \times 10^{-3}$	4.7(3)	$1.1(3) \times 10^{-1}$	3.0(15)	$4(1) \times 10^3$	Yes
12.141(1)	1526(3)	1^-	$1.0(2) \times 10^{-3}$	2.4(2)	1.7(5)	3.0(15)	$1.5(2) \times 10^4$	Yes
12.184(5)	1569(7)	0^+	$1.1(2) \times 10^{-3}$	$1.21(29) \times 10^1$	0.90(11)	3.0(15)	$3.3(5) \times 10^4$	Yes
12.270(5)	1658(7)	0^+	$8.9(1) \times 10^{-3}$	$2.1(2) \times 10^1$	$2.2(4) \times 10^2$	3.0(15)	$7.3(9) \times 10^4$	Yes
12.344(2)	1728(4)	0^+	$5.4(7) \times 10^{-2}$	$1.57(10) \times 10^2$	$6.30(12) \times 10^2$	3.0(15)	$3.5(5) \times 10^4$	Yes

Table II from: P. Adsley, *et al.*, Phys. Rev. C, **103** (2021) 015805

^{22}Ne(α, n) Part II: ^{26}Mg states w/ unmeasured Γ_α or $\omega\gamma$

- Known natural parity states that may contribute
- High resolution and sensitivity to Γ_α is needed

E_x (MeV)	E_r^{CM} (keV)	J^π	$\Gamma_{\alpha,UL}$ (eV)	Γ_γ (eV)	Γ_n (eV)	Integrate resonance?
10.6507(4)	36.0(4)	7^-	1.60×10^{-76}	3.0(15)	0	No
10.8057(7)	191.0(7)	1^-	3.2×10^{-23}	0.72(18)	0	No
10.818(1)	203(1)	0^+	1.29×10^{-20}	3.0(15)	0	No
10.826(1)	211(1)	(2^+)	6.65×10^{-21}	3.0(15)	0	No
10.8976(47)	278(1)	(4^+)	1.41×10^{-18}	3.0(15)	0	No
10.9491(1)	334.4(8)	1^-	2.90×10^{-15}	1.9(3)	0	No
11.11223(4)	497.49(5)	2^+	4.3×10^{-10}	$1.37(6) \times 10^{-2}$	$2.095(5) \times 10^3$	Yes
11.16310(4)	548.36(5)	2^+	5.2×10^{-9}	2.8(2)	$5.31(5) \times 10^3$	Yes
11.16926(4)	554.52(5)	3^-	4.4×10^{-10}	3.3(2)	$1.94(2) \times 10^3$	Yes
11.17107(4)	556.33(5)	2^+	1.3×10^{-11}	3(2)	0.8(7)	No
11.27380(4)	659.06(5)	2^+	1.00×10^{-6}	2.2(2)	$4.1(1) \times 10^2$	Yes
11.27963(4)	664.89(5)	3^-	9.20×10^{-8}	$3(1) \times 10^{-1}$	$1.81(2) \times 10^3$	Yes
11.30100(9)	686.26(9)	(2^+)	1.53×10^{-5}	<3	$<2.0 \times 10^1$	No
11.32768(4)	712.94(5)	(1^-)	1.80×10^{-6}	2.2(3)	$1.71(6) \times 10^2$	Yes
11.33696(4)	722.22(5)	(1^-)	1.74×10^{-4}	<3	$<2.0 \times 10^1$	No
11.34389(9)	729.15(9)	(2^+)	1.10×10^{-6}	1.0(2)	$<1.95 \times 10^3$	Yes
11.50022(4)	885.48(5)	1^-	1.95×10^{-1}	3.0(15)	$3.0(15) \times 10^3$	Yes

Table III from: P. Adsley, *et al.*, Phys. Rev. C, **103** (2021) 015805

what device can we use to help resolve this problem. . . ?

miniTPC at ELI-NP: In hand!

- Electronic Time Projection Chamber (TPC)
- Gas Electron Multiplier (GEM) foils
- Successfully commissioned with α beams (2018)
- Basically an ionization chamber: X, Y, Z, $(\Delta)E$
- Essentially 4π coverage for charged particles
- Active target volume: $105 \times 105 \times 200$ mm^3
- Neon is a suitable fill gas for this active target

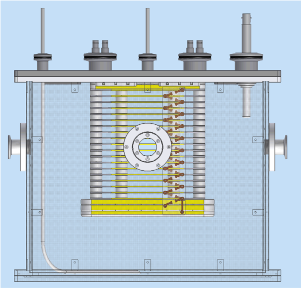

(a) Schematic

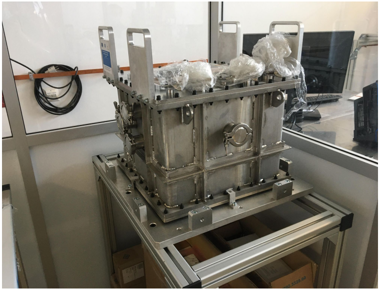

(b) Photograph

how can the miniTPC address the ^{22}Ne(α, n) reaction. . . ?

^{22}Ne(α, n) reaction rate by ^{22}Ne(^{6}Li, d), Part I

- The (^{6}Li, d) reaction is a known α-transfer to obtain Γ_α
  - $\gamma = \Gamma_\alpha \iff \Gamma_\alpha \ll \Gamma_n$; Γ_α controls the reaction rate
- Two recent studies in inverse kinematics of ^{6}Li(^{22}Ne, d)
  - Published in Phys. Lett. B (2020), with conflicting results
  - Lithium content of targets $< 10\ \mu g/cm^2$
  - Jayatissa *et al.* obtained 95 keV resolution
  - Ota *et al.* obtained 230 keV resolution
- Propose to measure in normal kinematics with miniTPC
  - Target thickness over mg/cm^2, 4π coverage
  - Several mm resolution, with $\Delta E \sim 10$ keV/mm

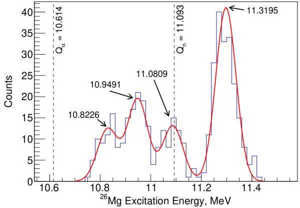

(a) 95 keV Resolution

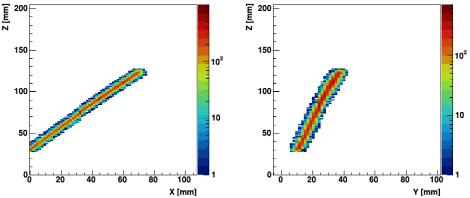

(b) α track in the miniTPC (thanks Warsaw)

some decisions need to be made after a test experiment...

^{22}Ne(α, n) reaction rate by ^{22}Ne(^{6}Li, d), Part II

- ^{6}Li at low energy: smaller σ, needs 10^7 pps beam
  - Unknown if the miniTPC can handle such intensity
  - Less target gas required to stop heavy recoils
  - Extracted data is less model dependent
- ^{6}Li at high energy: larger σ, needs 10^6 pps beam
  - More target gas required to stop heavy recoils
  - Extracted data is model dependent
- Priority requests (separated from physics machine time):
  - 2 days: ^{6}Li intensity check and energy loss calibration
  - 0.5 days: ^{24}Mg energy loss calibration: $E_{\text{beam}} < 15$ MeV

^{6}Li Beam Energy (MeV)	Cross Section (mb)
6.0	8.1103×10^{-4}
7.0	1.7163×10^{-3}
20.0	1.1970×10^{-2}
32.0	2.2368×10^{-2}
82.7	3.2228×10^{-2}

(a) $\sigma(E)$ from FRESCO

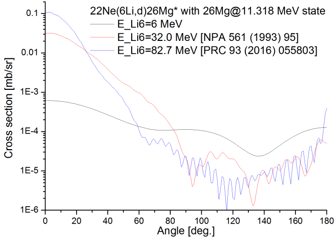

(b) Differential Cross Sections

^{22}Ne(α, n) reaction rate by ^{22}Ne(^{6}Li, d), Part III

- Thick target in normal kinematics: deutron escapes TPC
- Heavy recoil has similar energy deposit to the beam
  - Single dynamic range
  - Full angular coverage
  - Reaction location precisely measured $\rightarrow E_{\text{c.m.}}$
  - Q-value from ΔE-E clearly identifies contaminat processes
  - (^{6}Li, ^{6}Li) simultaneously for optical potential
- 4 days of machine time needed for statistics of Jayatissa
  - We request 8 days for newly resolved, weaker resonances
- This is a new and novel approach to the ^{22}Ne(α, n) reaction

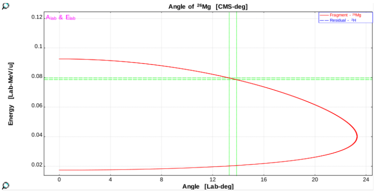

(a) ^{6}Li $E_{\text{beam}} = 7$ MeV

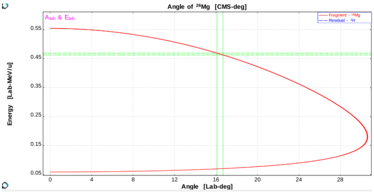

(b) ^{6}Li $E_{\text{beam}} = 32$ MeV

that's about it. . .


Thank you!